# Prion protein interacts with bace1 and differentially regulates its activity towards wild type and swedish mutant amyloid precursor protein

Neurobiology:

# Prion Protein Interacts with BACE1 Protein and Differentially Regulates Its Activity toward Wild Type and Swedish Mutant Amyloid Precursor Protein

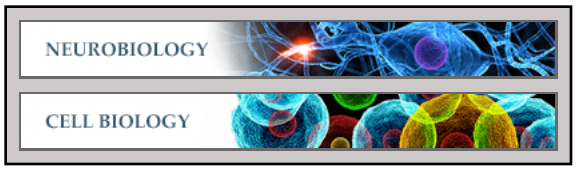


Heledd H. Griffiths, Isobel J. Whitehouse, Herbert Baybutt, Debbie Brown, Katherine A. B. Kellett, Carolyn D. Jackson, Anthony J. Turner, Pedro Piccardo, Jean C. Manson and Nigel M. Hooper

*J. Biol. Chem. 2011, 286:33489-33500.*
*doi: 10.1074/jbc.M111.278556 originally published online July 27, 2011*

---

THE JOURNAL OF BIOLOGICAL CHEMISTRY VOL. 286, NO. 38, pp. 33489–33500, September 23, 2011
Printed in the U.S.A.

# Prion Protein Interacts with BACE1 Protein and Differentially Regulates Its Activity toward Wild Type and Swedish Mutant Amyloid Precursor Protein*[S]

Received for publication, July 5, 2011 Published, JBC Papers in Press, July 27, 2011, DOI 10.1074/jbc.M111.278556

**Heledd H. Griffiths[‡], Isobel J. Whitehouse[‡], Herbert Baybutt[§], Debbie Brown[§], Katherine A. B. Kellett[‡], Carolyn D. Jackson[‡], Anthony J. Turner[‡], Pedro Piccardo[§¶], Jean C. Manson[§], and Nigel M. Hooper[‡1]**

*From the [‡]Institute of Molecular and Cellular Biology, Faculty of Biological Sciences, University of Leeds, Leeds LS2 9JT, United Kingdom, [§]The Roslin Institute and Royal (Dick) School of Veterinary Studies, University of Edinburgh, Roslin, Midlothian EH25 9PS, United Kingdom, and the [¶]Center for Biologics Evaluation and Research, Food and Drug Administration, Rockville, Maryland 20852*

**In Alzheimer disease amyloid-β (Aβ) peptides derived from the amyloid precursor protein (APP) accumulate in the brain. Cleavage of APP by the β-secretase BACE1 is the rate-limiting step in the production of Aβ. We have reported previously that the cellular prion protein ($PrP^C$) inhibited the action of BACE1 toward human wild type APP ($APP_{WT}$) in cellular models and that the levels of endogenous murine Aβ were significantly increased in $PrP^C$-null mouse brain. Here we investigated the molecular and cellular mechanisms underlying this observation. $PrP^C$ interacted directly with the prodomain of the immature Golgi-localized form of BACE1. This interaction decreased BACE1 at the cell surface and in endosomes where it preferentially cleaves $APP_{WT}$ but increased it in the Golgi where it preferentially cleaves APP with the Swedish mutation ($APP_{Swe}$). In transgenic mice expressing human APP with the Swedish and Indiana familial mutations ($APP_{Swe,Ind}$), $PrP^C$ deletion had no influence on APP proteolytic processing, Aβ plaque deposition, or levels of soluble Aβ or Aβ oligomers. In cells, although $PrP^C$ inhibited the action of BACE1 on $APP_{WT}$, it did not inhibit BACE1 activity toward $APP_{Swe}$. The differential subcellular location of the BACE1 cleavage of $APP_{Swe}$ relative to $APP_{WT}$ provides an explanation for the failure of $PrP^C$ deletion to affect Aβ accumulation in $APP_{Swe,Ind}$ mice. Thus, although $PrP^C$ exerts no control on cleavage of $APP_{Swe}$ by BACE1, it has a profound influence on the cleavage of $APP_{WT}$, suggesting that $PrP^C$ may be a key protective player against sporadic Alzheimer disease.**

A small minority (<1%) of Alzheimer disease (AD)[2] cases are inheritable and are caused by mutations in the genes encoding the amyloid precursor protein (APP), presenilin-1 (PS1), and PS2 (1). Specific examples include the Swedish familial AD double point mutation K670N/M671L in APP (2) and the Indiana familial AD point mutation V717F in APP (3). However, the underlying causes remain elusive for the majority of late onset sporadic AD cases. AD is characterized by the deposition in the brain of amyloid plaques composed primarily of the 40–42-amino acid amyloid-β (Aβ) peptide (4), which is derived from APP through sequential proteolytic cleavage by the β-secretase (β-site APP-cleaving enzyme-1 (BACE1)) and the PS1- or PS2-containing γ-secretase complex (5). Cleavage of APP at the $Met^{671}$-$Asp^{672}$ peptide bond by BACE1 is the first and rate-limiting step in the production of Aβ (6).

The activity of BACE1 is increased in the brain in sporadic AD and correlates with increased Aβ load (7, 8), suggesting a deregulation of normal homeostatic control mechanisms in the disease. The activity of BACE1 is regulated by a number of proteins (9), including the cellular prion protein ($PrP^C$) (10). $PrP^C$ inhibited the action of BACE1 toward human $APP_{WT}$ in cellular models, and the level of endogenous murine Aβ was significantly increased in the brain of $PrP^C$-null mice (10). Following this, we proposed that a normal function of $PrP^C$ may be to protect against AD (11). Consistent with this hypothesis is the observation that the level of $PrP^C$ is decreased in the hippocampus of sporadic, but not familial, AD subjects, indicating that the reduced level of $PrP^C$ is a primary mechanism of disease and is not a secondary consequence of AD-associated changes (12).

BACE1 is synthesized in the endoplasmic reticulum (ER) as an immature but catalytically active zymogen of approximately 60 kDa with an N-terminal prodomain (amino acids 22–45). Subsequent removal of the prodomain by furin-like convertases in the trans-Golgi network (TGN) along with other post-translational modifications transforms BACE1 into the mature protein of approximately 70 kDa (13–16). The mature BACE1 traffics from the TGN to the plasma membrane before being

* This work was supported, in whole or in part, by National Institutes of Health Agreement Y1-AI-4893-02 from the NIAID. This work was also supported by Medical Research Council of Great Britain Grants G9824728 and G0802189, Alzheimer's Research Trust of Great Britain Grant PG2008/2, and Food and Drug Administration Agreement 224-05-1307.

[S] The on-line version of this article (available at http://www.jbc.org) contains supplemental Fig. S1.

[1] To whom correspondence should be addressed. Tel.: 44-113-343-3163; Fax: 44-113-343-5638; E-mail: n.m.hooper@leeds.ac.uk.

[2] The abbreviations used are: AD, Alzheimer disease; Aβ, amyloid-β; APP, amyloid precursor protein; $APP_{Swe}$, APP with the Swedish mutation; $APP_{Swe,Ind}$, APP with the Swedish and Indiana familial mutations; $APP_{WT}$, wild type APP; BACE1, β-site APP-cleaving enzyme-1; BACE2, β-site APP-cleaving enzyme-2; ΔPD-rBACE1, BACE1 lacking the prodomain; EEA1, early endosomal antigen-1; ER, endoplasmic reticulum; $PrP^C$, cellular prion protein; PS, presenilin; rBACE1, recombinant BACE1; rPrP, recombinant PrP; sAPP, soluble APP; sAPPβ, soluble APP following β-secretase cleavage; TGN, trans-Golgi network; DPBS, Dulbecco's phosphate-buffered saline; CHAPSO, 3-[(3-cholamidopropyl)dimethylammonio]-2-hydroxy-1-propanesulfonic acid.

reinternalized into the endosomal pathway along with APP. It is within these acidic endosomal compartments that BACE1 primarily acts on wild type APP ($APP_{WT}$) (14, 17–19). In contrast to $APP_{WT}$, the $\beta$-secretase cleavage of APP with the Swedish mutation ($APP_{Swe}$) occurs primarily within the secretory pathway (20, 21).

In this study, we have extended our work on the role of $PrP^C$ in regulating BACE1 activity by determining the molecular and cellular mechanisms involved. We demonstrate that BACE1 coimmunoprecipitates with $PrP^C$ from murine and human brain and by surface plasmon resonance that $PrP^C$ interacts directly with the prodomain of BACE1. Site-directed mutagenesis revealed that $Pro^{29}$ in the prodomain of BACE1 is critical for this interaction. Furthermore, by immunofluorescence microscopy and fluorescence-activated cell sorting (FACS), we show that this interaction with the prodomain-containing form of BACE1 retains the secretase in the TGN and inhibits its trafficking to the cell surface and endosomes. As our previous data indicated that $PrP^C$ functions upstream of A$\beta$ production, we also examined the effect of $PrP^C$ deletion on A$\beta$ production and deposition in a transgenic mouse model expressing human APP with the Swedish and Indiana familial mutations ($APP_{Swe,Ind}$). Although deletion of $PrP^C$ had no effect on amyloid deposition in these transgenic mice, in a cellular model, we demonstrate that $PrP^C$ did not inhibit the activity of BACE1 toward $APP_{Swe}$ but did inhibit the activity of BACE1 toward $APP_{WT}$. As $APP_{Swe}$ is preferentially cleaved by BACE1 in the TGN rather than in endosomes as for $APP_{WT}$, this substrate-specific differential subcellular site of action of BACE1 provides a molecular explanation for the lack of effect of $PrP^C$ on A$\beta$ production and deposition in the $APP_{Swe,Ind}$ transgenic mice.

## EXPERIMENTAL PROCEDURES

*Coimmunoprecipitation*—Frozen human brain tissue was obtained from the Medical Research Council London Neurodegenerative Diseases Brain Bank (Institute of Psychiatry, King's College London). All materials were obtained with informed consent and approval of the relevant local ethics committees. All subsequent experiments were performed with the approval of the Leeds (Central) Research Ethics Committee. Human hippocampal brain tissue from a non-demented individual (male; age, 57; cause of death, left ventricular failure; post-mortem delay, 45 h) and 129/Ola wild type mice (22) (age, 5 weeks) were homogenized in 9 volumes of phosphate-buffered saline (PBS; without $Ca^{2+}$ and $Mg^{2+}$), 0.5% (v/v) Nonidet P-40, 0.5% (w/v) sodium deoxycholate, pH 7.4 in the presence of Complete protease inhibitor mixture (Roche Applied Science) using an electric homogenizer. Samples were centrifuged at 14,000 $\times$ *g* for 10 min, and the protein content of the resultant supernatant was quantified using bicinchoninic acid. Mouse or human brain homogenate (300 $\mu$g) was precleared using 0.5% (w/v) protein G-Sepharose (Sigma) for 30 min at room temperature. The protein G-Sepharose was pelleted by centrifugation at 14,000 $\times$ *g* for 20 s, and the supernatant was incubated in the presence or absence of 0.1% (v/v) of the PrP-specific antibody 6H4 (Prionics AG, Zurich, Switzerland) overnight at 4 °C. Protein G-Sepharose (0.5% (w/v)) was added to the samples and incubated for 1 h at room temperature. The immunocomplexes were pelleted by centrifugation at 14,000 $\times$ *g* for 20 s; washed three times with 10 mM potassium acetate, 1.5 mM $MgCl_2$, 75 mM sodium citrate; and subjected to immunoblotting.

*SDS-PAGE and Immunoblotting*—Proteins were resolved by SDS-PAGE using either 7–17% polyacrylamide gradient, 10%, or 14.5% polyacrylamide gels and transferred to Immobilon P polyvinylidene difluoride (PVDF) membrane (Amersham Biosciences). The membrane was blocked by incubation for 1 h with PBS containing 0.1% (v/v) Tween 20 and 5% (w/v) dried milk powder. Antibody incubations were performed in PBS-Tween 20 containing 2% (v/v) BSA. The following antibodies were used. 3F4 and 6D11 (both Eurogentec Ltd., Southampton, UK) and SAF32 (Cayman Chemical, Ann Arbor, MI) recognize $PrP^C$, 22C11 (Millipore Ltd., Livingston, UK) recognizes APP, and AC-15 recognizes actin (Sigma). 1A9 raised against a neoepitope formed on wild type sAPP$\beta$ following $\beta$ cleavage of APP and the antibody recognizing the neoepitope on Swedish sAPP$\beta$ were kindly provided by Dr. I. Hussain (GlaxoSmith-Kline, Harlow, UK). EE-17 (Sigma-Aldrich) recognizes residues 46–61 of BACE1. BACE-Cat1 raised against the BACE1 catalytic domain was kindly provided by Dr. R. Vassar (23). Antibody against the prodomain of BACE1 (residues 26–45) was from Merck Chemicals Ltd., and antibody against BACE2 was from Abcam (Cambridge, UK). Antibodies against the A$\beta$-degrading enzymes neprilysin (R&D Systems, Inc.) and insulin-degrading enzyme (Abcam) and antibodies against the synaptic markers synaptophysin (Synaptic Systems GmbH), PSD95 (Synaptic Systems GmbH), and drebrin (MBL International Corp., Woburn, MA) were from the sources indicated. Antibody against the $\gamma$-secretase complex components nicastrin was from Abcam, and antibody against presenilin-1 N-terminal fragment was from Covance (Cambridge, UK). Horseradish peroxidase (HRP)-conjugated secondary antibodies were used at 1:4000 in the same buffer. Bound antibody was detected using the enhanced chemiluminescence detection method (Amersham Biosciences). Blots were stripped using 100 mM glycine, pH 2.5 for 30 min, blocked by incubation for 1 h with PBS containing 0.1% (v/v) Tween 20 and 5% (w/v) dried milk powder, and reprobed using the anti-actin antibody as described above. Anti-Fc-HRP was diluted in PBS-Tween 20.

*BACE1 ELISA*—96-well plates (BD Biosciences) were coated overnight with murine recombinant PrP (rPrP) (Allprion AG, Schlieren, Switzerland) (20 pmol/well; 5 $\mu$g/ml). The plates were washed with washing buffer (Dulbecco's phosphate-buffered saline (DPBS) containing 0.05% (v/v) Tween 20 and 0.02% (w/v) sodium azide) before being blocked for 2 h in 3% (w/v) BSA diluted in DPBS containing 0.02% (w/v) sodium azide. The plates were then incubated with various concentrations (0–20 pmol) of recombinant BACE1-Fc (a kind gift from Dr. R. Matico, GlaxoSmithKline, Collegeville, PA) or recombinant Thy1-Fc (Alexis Biochemicals, Lausen, Switzerland) for 2 h. Residual material was washed away, and the plate was incubated with anti-Fc-HRP (1:5000) for 2 h. Bound protein was detected using 3,3′,5,5′-tetramethylbenzidine reagent (Kirkegaard & Perry Laboratories, Inc., Gaithersburg, MD) and allowed to develop for 30 min prior to the addition of 1 M $H_3PO_4$ to stop

the reaction. The absorbance was then measured at 450 nm on an Anthos plate reader.

*Surface Plasmon Resonance*—All reagents and systems used in this technique were obtained from Amersham Biosciences. Surface plasmon resonance was performed on Biacore 3000 system. A carboxymethyldextran chip (CM5) was primed with running buffer (DPBS, 0.005% Tween 20) and normalized using BIAnormalizing solution (70% (w/v) glycerol). rPrP (10 $\mu$g/ml in 10 mM sodium acetate, pH 4.5) was immobilized to the chip at a rate of 5 $\mu$g/min for 7 min to a level of 1500 resonance units (RU) by amine coupling. Recombinant rBACE1-Fc and ΔPD-rBACE1 obtained from pepsin digestion of the rBACE1-Fc (provided by Dr. R. Matico, GlaxoSmithKline, Collegeville, PA) were diluted in running buffer to a range of concentrations (0–10,000 nM) and passed over the sensor chip surface at a flow rate of 40 $\mu$l/min. Each cycle consisted of a 300-s analyte injection (association phase) followed by a 300-s dissociation phase. Regeneration was not necessary, but a 300-s stabilization period was applied. The data were analyzed using Biacore evaluation software (BIAevaluation 3.2RC1). Base lines were adjusted to zero for all curves and double referenced by subtracting a sensorgram of buffer injected over the rPrP surface from the experimental sensorgrams to give the curves representing specific binding. Curves were modeled assuming a simple 1:1 interaction to generate kinetic data. The $\chi^2$ value was below 5 RU$^2$, indicating a good fit to the binding model.

*Fluorometric BACE1 Activity Assay*—Membrane fractions (10 $\mu$g) were diluted in 100 mM sodium acetate, pH 4.5, 40 mM NaCl, 10% (v/v) glycerol, 0.2% CHAPS, 1 mM EDTA, protease inhibitor mixture (P8340, Sigma-Aldrich). The samples were incubated in the presence or absence of $\beta$-secretase inhibitor IV (Merck Chemicals Ltd.) for 30 min at 37 °C before addition of the quenched fluorescence peptide based on the APP$_{Swe}$ sequence (FAM-ISEVNLDAEFR-TAMRA where FAM is carboxyfluorescein and TAMRA is carboxytetramethylrhodamine; GlaxoSmithKline, Stevenage, UK) (5 $\mu$M) in 100 mM sodium acetate, pH 4.5, 0.06% Triton X-100. The fluorescence was then measured on a Synergy HT Bio-Tek fluorometer using KC4 software with excitation and emission wavelengths set to 485 and 585 nm, respectively.

*Site-directed Mutagenesis and Stable Transfection*—BACE1 mutants were generated from the template cDNA encoding human BACE1 in pIRES*hyg* using the QuikChange II XL site-directed mutagenesis kit (Stratagene, Cambridge, UK) with the following primers (Eurogentec Ltd.) (mutant bases are indicated in bold): For L28Q/L30Q mutant, the sense primer was 5′-GCATCCGGC**A**GCCCC**A**GCGCAGCGG-3′, and the antisense primer was 5′-CCGCTGCGC**T**GGGGC**T**GCCGGATGC-3′. For P29G mutant, the sense primer was 5′-GGCATCCGGCTG**GG**CCTGCGCAGCGG-3′, and the antisense primer was 5′-CCGCTGCGCAGG**CC**CAGCCGGATGCC-3′. For APP$_{Swe}$, the sense primer was 5′-CGGAGGAGATCTCTGAAGTGAA**TT**TGGATGCAGAATTCCGA-3′, and the antisense primer was 5′-TCGGAATTCTGCATCCA**AA**TTCACTTCAGAGATCTCCTCCG-3′. The resultant constructs were verified by DNA sequencing. cDNA encoding the human BACE1 mutants, BACE2, and APP$_{Swe}$ in the expression vector pIRES*hyg* were introduced by electroporation into human embryonic kidney (HEK) cells expressing murine PrP$^C$ (containing the 3F4 epitope tag at amino acids 108–111) (24) in the expression vector pIRES*neo* or into cells expressing pIRES*neo* expression vector only as a control. Cells were selected using 150 $\mu$g/ml hygromycin B. SH-SY5Y cells were stably transfected with cDNA encoding BACE1 and PrP$^C$ as described previously (10).

*Cell Culture*—Human neuroblastoma (SH-SY5Y) and HEK cells were cultured in Dulbecco's modified Eagle's medium containing 4.5 g/liter glucose with 2 mM L-glutamine supplemented with 50 units/ml penicillin and 0.1 mg/ml streptomycin (Lonza) and 10% (v/v) fetal bovine serum (FBS) (Sigma-Aldrich). Cells were maintained in a humid atmosphere at 37 °C containing 5% (v/v) $CO_2$ in air. All cell lines were grown to 100% confluence and washed twice in DPBS (without $Ca^{2+}$ and $Mg^{2+}$) prior to a 24-h incubation in Opti-MEM and GlutaMAX (Invitrogen). Medium was harvested and stored at −20 °C for use in the A$\beta$ ELISA or concentrated to 200 $\mu$l in a Vivaspin 20-ml concentrator (10,000 molecular weight cutoff membrane) centrifuged at 1900 × *g* for ~1 h in a bench top centrifuge maintained at 4 °C. For analysis of cell-associated proteins, cells were washed in DPBS, scraped, and pelleted at 1400 × *g* for 3 min. Cells were lysed in 50 mM Tris/HCl, 150 mM NaCl, 0.5% (w/v) sodium deoxycholate, 1% (v/v) Nonidet-P40, pH 8.0. For the preparation of membranes, cells were resuspended in 3 ml of 50 mM HEPES, pH 7.5 and sonicated at an amplitude of 7 $\mu$m for 30 s using a Soniprep150. The cell suspension was then centrifuged at 2500 × *g* for 10 min at 4 °C to pellet cell membranes and nuclei. The supernatant was then centrifuged in a Beckman Coulter Optima at 100,000 × *g* for 1 h at 4 °C. Membranes were resuspended in 50 mM Tris/HCl, pH 7.5, 2 mM EDTA, 150 mM NaCl, 1% (w/v) CHAPSO.

*siRNA Transfection*—siRNAs corresponding to the human *PRNP* gene were synthesized by Thermo Scientific Dharmacon (Sussex, UK) as ON-TARGET plus SMARTpool. The sequences of the siRNAs are as follows: UCACCGAGACCGACGUUAA, GAUCGAGCAUGGUCCUCUU, AGAUGUGUAUCACCCAGUA, and GACCGUUACUAUCGUGAAA. HEK293 cells were seeded at 60–70% confluence in a T80 flask 24 h before transfection. siRNA (1 $\mu$M of the stock solution) was mixed with the corresponding half-volume of Dharmafect 1 reagent in Opti-MEM (Invitrogen) for 20 min and applied to the cells in a final volume made up to 5 ml with DMEM supplemented with 10% FBS. After incubation for 48 h at 37 °C, cells were washed with PBS, and medium was conditioned for 24 h.

*Immunofluorescence Microscopy*—Cells grown on coverslips were fixed with 4% (v/v) paraformaldehyde for 10 min and then permeabilized in DPBS containing 0.1% (v/v) Triton X-100 or fixed and permeabilized in ice-cold 50% (v/v) methanol, 50% (v/v) acetone for 10 min. Coverslips were incubated in DPBS containing 5% (v/v) fish skin gelatin (Sigma-Aldrich) for 3–4 h at room temperature before being incubated overnight at 4 °C with the following primary antibodies: EE-17 against BACE1, 3F4 against PrP$^C$, a mouse monoclonal antibody against early endosomal antigen-1 (EEA1; BD Biosciences Pharmingen), a sheep polyclonal antibody against the trans-Golgi network protein-46 (TGN-46; a kind gift from Dr. V. Ponnambalam, University of Leeds, Leeds, UK), and a chicken polyclonal antibody

against calreticulin (Abcam). Finally, coverslips were incubated with the appropriate fluorescent probe-conjugated secondary antibodies (Jackson ImmunoResearch Laboratories Inc. and Invitrogen) for 1 h and mounted on slides using Fluoromount-G mounting medium (SouthernBiotech). Individual cells were visualized using a DeltaVision Optical Restoration Microscopy System (Applied Precision Inc.). Data were collected from 20 0.1-$\mu$m-thick optical sections, and three-dimensional data sets were deconvolved using the SoftWoRx program (Applied Precision Inc.). Where indicated, the presented images represent individual Z-slices. Colocalization of BACE1 with intracellular markers was performed using ImageJ.

*FACS*—SH-SY5Y cell suspensions were diluted to $5 \times 10^6$ cells/ml with DPBS containing 2.5 mM EDTA, pH 8 (DPBS/EDTA buffer) and blocked for 20 min in 2% (v/v) fish skin gelatin diluted in DPBS/EDTA buffer. A 1 in 50 dilution of EE-17 was added to half the samples and incubated for 1 h. Following this, cell suspensions were washed twice and centrifuged at $10,000 \times g$ for 5 min before being resuspended in 2% (v/v) fish skin gelatin diluted in DPBS/EDTA buffer containing fluorescently conjugated secondary antibody (1:200) for 1 h. The cells were then washed as described above and resuspended in DPBS/EDTA buffer. Cells were sorted using a Partec PASIII (Partec UK Ltd., Kent, UK), and data were analyzed using WinMDI software version 2.9, or cells were sorted using a BD-LSR-Fortessa (BD Biosciences), and data were analyzed using BD FACSDiva software.

*Transgenic Animals*—Transgenic $APP_{Swe,Ind}$ mice overexpressing human APP with the Swedish (K670N/M671L) and Indiana (V717F) familial AD mutations (line J20) (25) were obtained from The Jackson Laboratory (Line B6.Cg-Tg(PDGFB-APPSwInd)20Lms/2J, stock number 006293) and The J. David Gladstone Institutes (San Francisco, CA) and crossed with inbred PrP knock-out mice (129Ola $PrP^{-/-}$) (22). All the transgenic mice used in this study were genotyped. DNA was prepared from ear punch tissue using a DNeasy kit (Qiagen). PCR was performed using the protocol specific for these mice from The Jackson Laboratory. Brain hemispheres were either frozen at −80 °C for biochemical analysis or fixed in 10% formol saline for histopathological analysis. Animal care was in accordance with institutional guidelines.

Fixed brain tissue was processed, and tissue sections were prepared as described (26). Paraffin sections (6 $\mu$m) were immunostained with a series of antibodies. The following antibodies were used: 4G8 (1:100) monoclonal antibody raised against A$\beta$(17–24) (Abcam), A11 (1:1000) anti-prefibrillar oligomer polyclonal antibody (AB9234, Millipore, Watford, UK), OC (1:5000) anti-fibrillar oligomer polyclonal antibody (a gift from Professor C. Glabe, Department of Neurology, University of California at Irvine School of Medicine, Irvine, CA), drebrin (10 $\mu$g/ml) monoclonal antibody to detect dendritic spines (D029-3, MBL International Corp.), synaptophysin (Envision kit K4001) polyclonal antibody to presynaptic vesicle protein (N1566, Dako, Cambridgeshire, UK), anti-glial fibrillary acidic protein (1:400) polyclonal antibody (Z0334, Dako), and Iba (1:1000) polyclonal antibody, a microglial marker (01-1974, Wako Chemicals USA, Inc.). Amyloid plaques were visualized with 1% thioflavin S (Sigma).

Brain hemispheres were homogenized using a two-step extraction protocol (27). Briefly, initial homogenization (120 mg/ml wet weight) was carried out using an electric homogenizer in 2% (w/v) SDS containing protease mixture inhibitor (Roche Diagnostics GmbH) followed by centrifugation at $100,000 \times g$ for 1 h at 4 °C. The resultant supernatant was collected and analyzed using the A$\beta$ ELISA and SDS-PAGE followed by immunoblotting. The pellet was extracted in 70% (v/v) formic acid in distilled $H_2O$ followed by centrifugation at $100,000 \times g$ for 1 h at 4 °C. The supernatant was collected and analyzed using the A$\beta$ ELISA.

*A$\beta$ ELISA*—Sandwich ELISAs for the detection of human A$\beta$(1–40) and A$\beta$(1–42) were performed as described previously (28). Briefly, 96-well microtiter plates were coated overnight at 4 °C with primary antibodies against A$\beta$(1–40) (33.1.1) and A$\beta$(1–42) (2.1.3.35.86) (kind gifts from C. & L. Eckman, Mayo Clinic, Jacksonville, FL). Following blocking and incubation with conditioned medium, SDS-extracted brain homogenate, or formic acid-extracted brain homogenate, bound A$\beta$ peptides were detected with HRP-conjugated detection antibody (for A$\beta$(1–40), 13.1.1-HRP (C. & L. Eckman); for A$\beta$(1–42), 4G8-HRP (Covance)).

*Statistical Analysis*—Densitometric analysis was performed using the advanced image data analyzer (AIDA) program (Raytest Scientific Ltd.). The non-parametric two-tailed Mann-Whitney *U* test was used to compare two independent samples when sample numbers were less than $n = 6$. For sample numbers of $n \geq 6$, the Kolmogorov-Smirnov test was used to test that the data in each group were normally distributed. Following this, Levene's test was used to ensure that the data sets were of equal variance. In samples where the data met the criteria of a normal distribution and equal variance, the parametric independent *t* test was used to calculate significance. $p \leq 0.05$ was considered significant (*, $p < 0.05$; **, $p < 0.005$; error bars, ±S.E.). The data were analyzed using the Statistical Package for Social Sciences (SPSS 12.0.1) program (Chicago, IL).

## RESULTS

PrP$^C$ directly interacts with the prodomain of BACE1. Previously, we reported that BACE1 coimmunoprecipitated with PrP$^C$ in SH-SY5Y cells (10), although it remained to be established whether this was due to a direct protein-protein interaction. Initially, we extended this observation by examining whether the two endogenous proteins interacted in the brain. BACE1 coimmunoprecipitated with PrP$^C$ in both murine and human brain (Fig. 1*A*), providing further evidence that the interaction between the two proteins is physiological. Then, to investigate whether this was a direct protein-protein interaction, we utilized an ELISA system using recombinant proteins. Recombinant human BACE1 with an Fc tag at the C terminus (rBACE1-Fc; Fig. 1, *B* and *C*) bound specifically to immobilized rPrP (Fig. 1*D*). In contrast to rBACE1-Fc, a control Fc-tagged form of human Thy1 (rThy1-Fc) did not interact with the immobilized rPrP to the same extent (7.4-fold less bound at the highest concentration tested) (Fig. 1*D*), indicating that the PrP-BACE1 interaction was specific. Next, we utilized surface plasmon resonance to interrogate further the interaction between

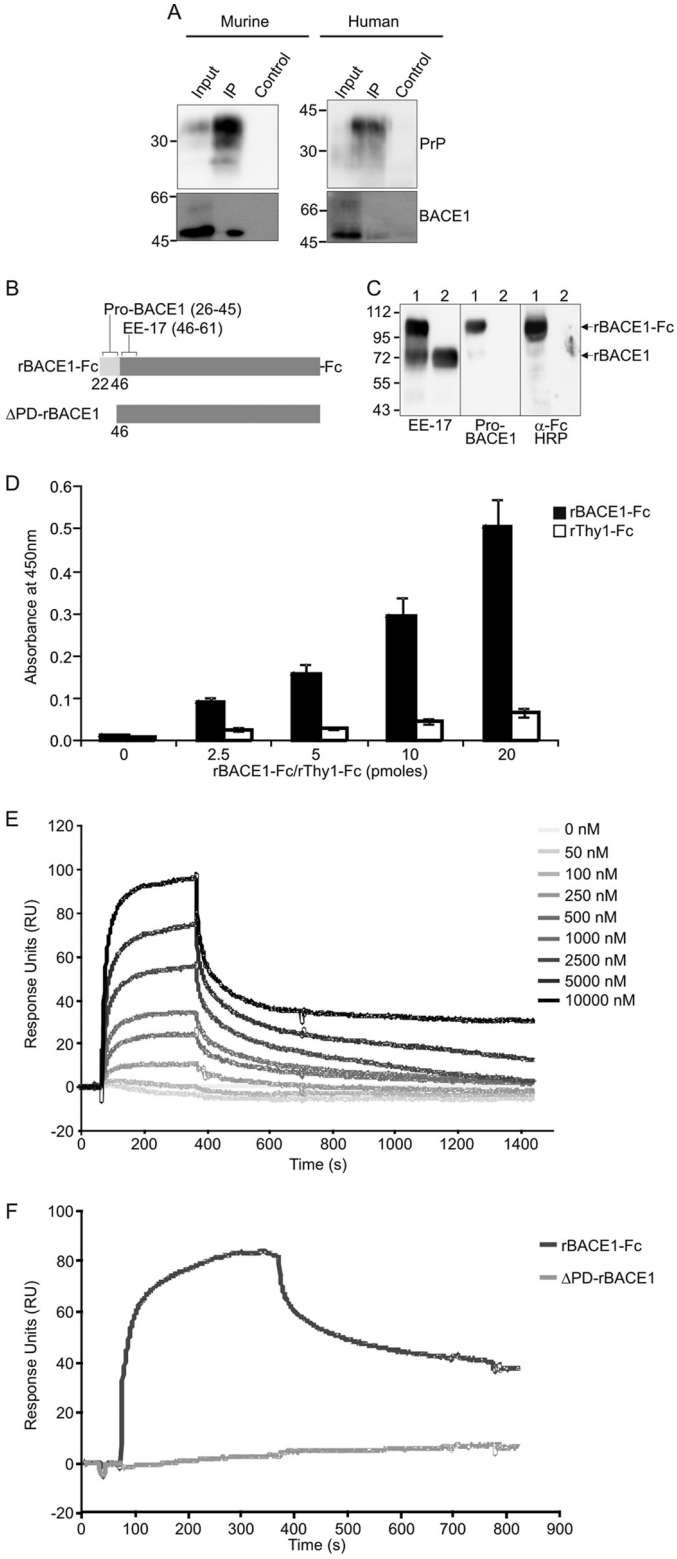


FIGURE 1. **PrP directly interacts with prodomain of BACE1.** *A*, brain homogenates from 129/Ola wild type mice and a non-demented individual were immunoprecipitated in the presence (*IP*) or absence (*Control*) of 6H4, and the immunoprecipitates were subjected to SDS-PAGE and immunoblotting alongside total brain homogenate (*Input*) with antibody SAF32 for murine and 3F4 for human PrP$^C$ and antibody EE-17 for BACE1. *B*, schematic of the prodomain-containing (rBACE1-Fc) and prodomain-lacking (ΔPD-rBACE1) BACE1 showing the epitopes recognized by antibody EE-17 and the prodomain antibody (*pro-BACE1*). *C*, rBACE1-Fc (*lane 1*) and ΔPD-rBACE1 (*lane 2*) immunoblotted with EE-17, prodomain antibody (*pro-BACE1*), or anti-Fc-HRP. *D*, rPrP was immobilized and incubated with rBACE1-Fc or rThy1-Fc before detection with anti-Fc-HRP ($n = 3$). *E*, rPrP was immobilized onto the surface of a CM5 sensor chip, and rBACE1-Fc was passed over the surface. The response from the reference was subtracted, and the base lines were adjusted to zero to give response over time binding curves. *F*, rBACE1-Fc (2500 nM) and ΔPD-rBACE1 (2500 nM) were passed over the rPrP-immobilized sensor chip. *Error bars*, ±S.E.

PrP$^C$ and BACE1. rBACE1-Fc bound to the immobilized rPrP in a dose-dependent manner with a $K_d$ of 3.19 $\mu$M (Fig. 1*E*).

The coimmunoprecipitation studies indicated that PrP$^C$ was interacting with the lower molecular weight immature form of BACE1 (Fig. 1*A*) (10). The rBACE1-Fc used in the above studies contains the prodomain as evidenced by its reactivity to an antibody raised against residues 26–45 in the prodomain (Fig. 1, *B* and *C*). Therefore, to determine whether PrP$^C$ was indeed interacting with the prodomain of BACE1, we utilized a form of BACE1 lacking the prodomain (ΔPD-rBACE1) that migrated on SDS-PAGE as a single band at ~62 kDa and was no longer recognized by the prodomain antibody (Fig. 1*C*). N-terminal sequencing confirmed that ΔPD-rBACE1 indeed lacked the prodomain, beginning at residue 46. ΔPD-rBACE1 displayed a specific activity toward a quenched fluorescent peptide substrate similar to that of the original prodomain containing rBACE1-Fc (11.73 and 12.4 units/min/$\mu$g of protein, respectively), consistent with reports that the prodomain does not inhibit the catalytic activity of the enzyme (15, 16). Using surface plasmon resonance, ΔPD-rBACE1 was observed not to bind to the immobilized rPrP (Fig. 1*F*). Together, these data indicate that the N-terminal prodomain of BACE1 (residues 22–45) is required for the direct interaction between BACE1 and PrP$^C$.

*Pro$^{29}$ in Prodomain of BACE1 Is Critical for Interaction with PrP$^C$*—To gain further insight into the direct interaction between BACE1 and PrP$^C$, we investigated whether PrP$^C$ would inhibit the action of the homolog of BACE1, BACE2. BACE2 shares 45% sequence identity with BACE1 and also cleaves APP albeit at the Phe$^{19}$-Phe$^{20}$ bond in the A$\beta$ sequence (29, 30). Upon coexpression in HEK293 cells, PrP$^C$ significantly inhibited the action of BACE2 on APP$_{WT}$ (Fig. 2, *A* and *B*). As PrP$^C$ inhibits both BACE1 and BACE2, we identified a conserved sequence (LPLR) in the prodomains of both proteins (Fig. 2*C*) that we interrogated in BACE1 by site-directed mutagenesis. L28Q/L30Q and P29G mutants were coexpressed in HEK293 cells with PrP$^C$. The P29G mutant was expressed at a level similar to that of the wild type BACE1 with the majority being complex glycosylated and appearing as the 75-kDa mature form (Fig. 2*D*), whereas the L28Q/L30Q mutant was predominantly (~90%) expressed as the 65-kDa immature ER form (Fig. 2*D*). The P29G mutant had an activity toward the quenched fluorescent peptide substrate similar to that of wild type BACE1 (Fig. 2*E*). As the L28Q/L30Q mutant did not appear to traffic through the secretory pathway correctly being present mainly as the immature ER form (Fig. 2*F*) and did not efficiently fold into a fully catalytically active form (Fig. 2*E*), it was not studied further. The prodomain containing a complex glycosylated immature form of BACE1 (~75 kDa) was increased in the presence of PrP$^C$ in the wild type BACE1-expressing cells but not in the P29G-expressing cells (Fig. 2, *F* and *G*). In the wild type

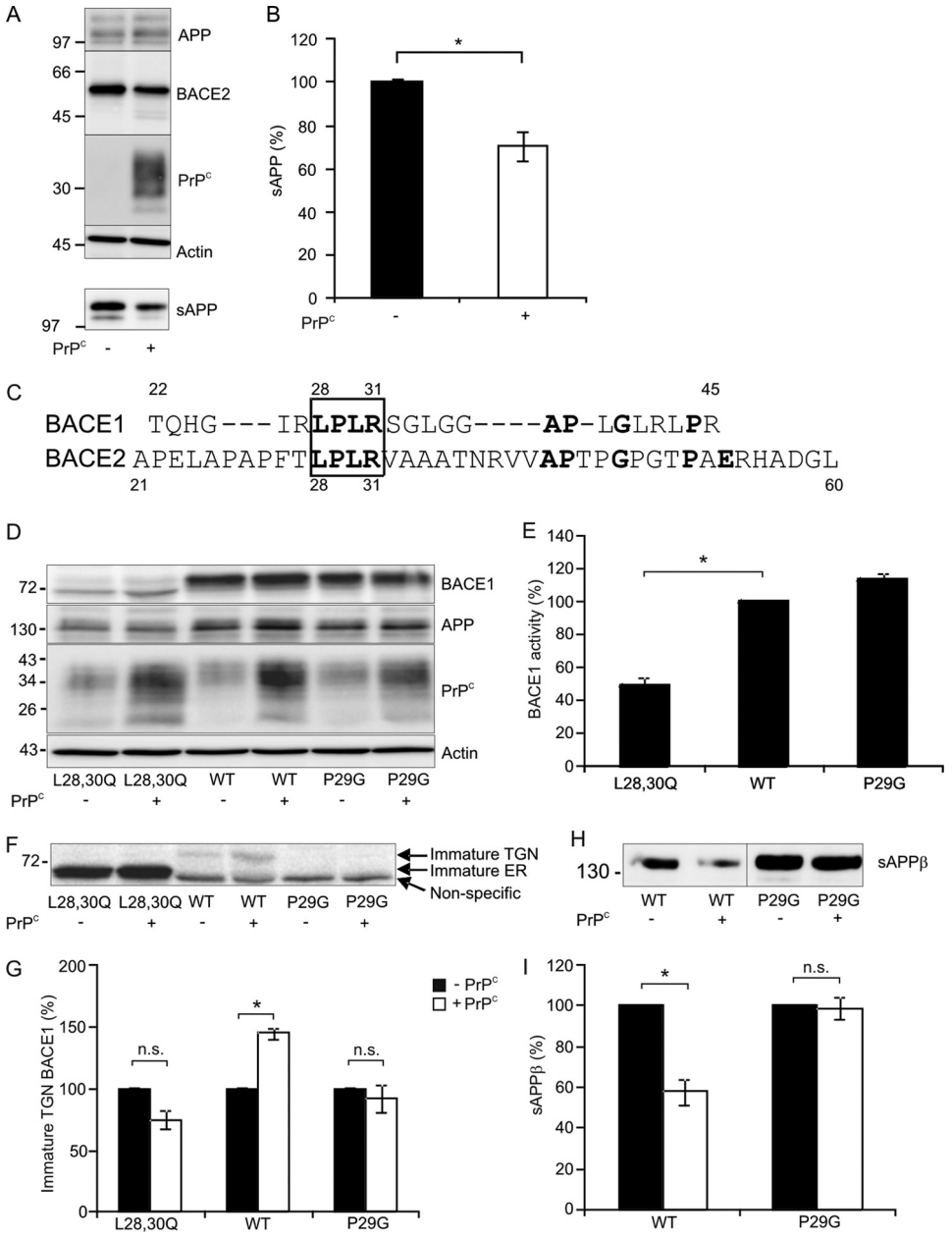


FIGURE 2. **Identification of binding site for PrP in BACE1 prodomain.** *A*, lysates from HEK293 cells expressing BACE2 in the presence or absence or PrP$^C$ were subjected to SDS-PAGE and immunoblotting to detect APP$_{WT}$, BACE2, PrP$^C$, and actin. Medium samples were blotted for sAPP. *B*, quantification of multiple sAPP blots from HEK cells expressing BACE2 ($n = 3$). *C*, sequence alignment of the prodomains of BACE1 and BACE2. The LPLR conserved region is *boxed*. *D*, lysates from HEK293 cells expressing either L28Q/L30Q BACE1, WT BACE1, or P29G BACE1 in the presence or absence of PrP$^C$ were subjected to SDS-PAGE and immunoblotting to detect total BACE1, PrP$^C$, APP, and actin. *E*, BACE1 activity toward the synthetic peptide substrate in membranes from the HEK293 cells. The percentage of activity of the mutants was calculated relative to WT BACE1. *F*, amount of immature BACE1 (detected with the prodomain-specific antibody) in membranes. *G*, quantification by densitometric analysis of multiple immunoblots of the immature TGN form of BACE1 in the presence or absence of PrP$^C$ ($n = 5$). *H*, amount of sAPP$\beta$ in the conditioned medium. *I*, ratio of sAPP$\beta$ relative to total BACE1 for the WT BACE1- and P29G-expressing cells in the absence or presence of PrP$^C$ ($n = 3$). *, $p < 0.05$; *n.s.*, not significant; *error bars*, ±S.E.

BACE1-expressing cells, coexpression of PrP$^C$ significantly reduced the amount of sAPP$\beta$ in the conditioned medium derived from the endogenous human APP$_{WT}$, whereas PrP$^C$ failed to inhibit the amount of sAPP$\beta$ secreted from the P29G-expressing cells (Fig. 2, *H* and *I*). These data indicate that PrP$^C$ is interacting with the prodomain of BACE1 and that Pro$^{29}$ is critical for this interaction. Furthermore, these observations suggest that this interaction with PrP$^C$ prevents the removal of the prodomain, thus influencing the proportion of BACE1 that is cleaved to generate the mature form.

*PrP$^C$ Alters Subcellular Localization of BACE1*—Next, we investigated whether this interaction between PrP$^C$ and the prodomain of BACE1 altered the subcellular location of BACE1 by assessing whether the colocalization of BACE1 with various subcellular markers was altered by PrP$^C$. In SH-SY5Y cells, immunofluorescence microscopy revealed that PrP$^C$ caused a significant reduction (28.9 ± 4.7%, $p = 0.025$) in the colocalization of BACE1 with the early endosomal marker EEA1 (Fig. 3, *A* and *B*) and as assessed by FACS reduced the amount of BACE1 at the cell surface by 28.2 ± 9.1% ($p = 0.015$) (Fig. 3, *C* and *D*).

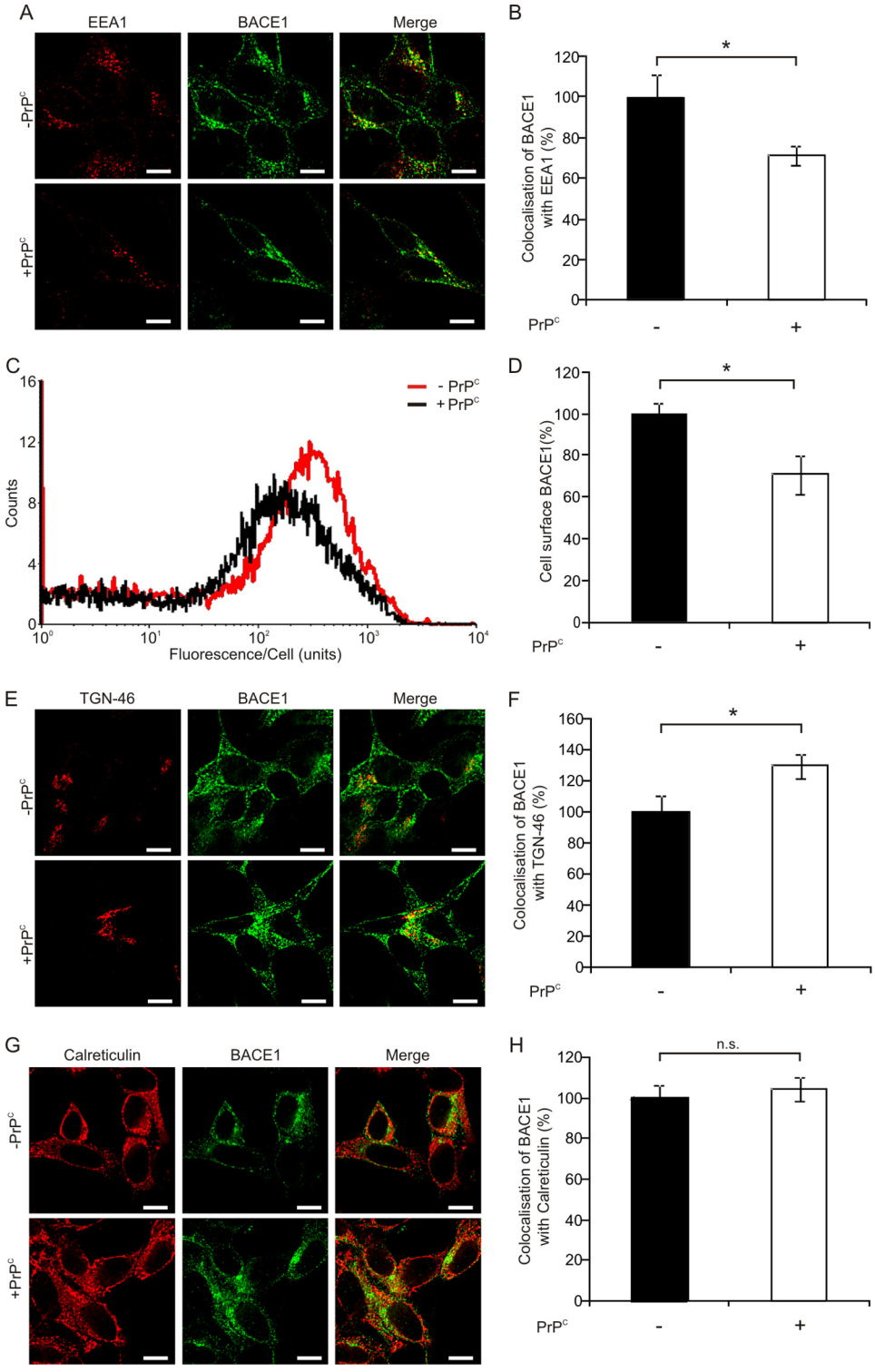


FIGURE 3. **PrP$^C$ alters subcellular localization of BACE1.** *A*, BACE1 and EEA1 staining of SH-SY5Y cells expressing BACE1 in the presence or absence of PrP$^C$. *B*, ImageJ analysis of BACE1 and EEA1 colocalization in SH-SY5Y cells in the presence or absence of PrP$^C$. The percentage of colocalization was calculated over 13 images. *C*, BACE1 cell surface fluorescence in the presence or absence of PrP$^C$ determined by FACS analysis. *D*, quantitation from FACS analysis of BACE1 surface fluorescence in the presence or absence of PrP$^C$ ($n = 9$). *E*, BACE1 and TGN staining in the presence or absence of PrP$^C$. *F*, ImageJ analysis of BACE1 and TGN-46 colocalization in SH-SY5Y cells in the presence or absence of PrP$^C$. The percentage of colocalization was calculated over 13 images. *G*, BACE1 and calreticulin staining in the presence or absence of PrP$^C$. *H*, ImageJ analysis of BACE1 and calreticulin colocalization in SH-SY5Y cells in the presence or absence of PrP$^C$. The percentage of colocalization was calculated over 12 images. *Scale bar*, 10 $\mu$m. *, $p < 0.05$; *n.s.*, not significant; *error bars*, $\pm$S.E.

As both the cell surface and endosomal localization of BACE1 was reduced in the presence of PrP$^C$, we investigated whether PrP$^C$ was retaining BACE1 within the secretory pathway. Immunofluorescence microscopy revealed that PrP$^C$ significantly increased (29.4 $\pm$ 7.6%, $p = 0.028$) the colocalization of BACE1 with the TGN-specific protein TGN-46 (Fig. 3, *E* and *F*)

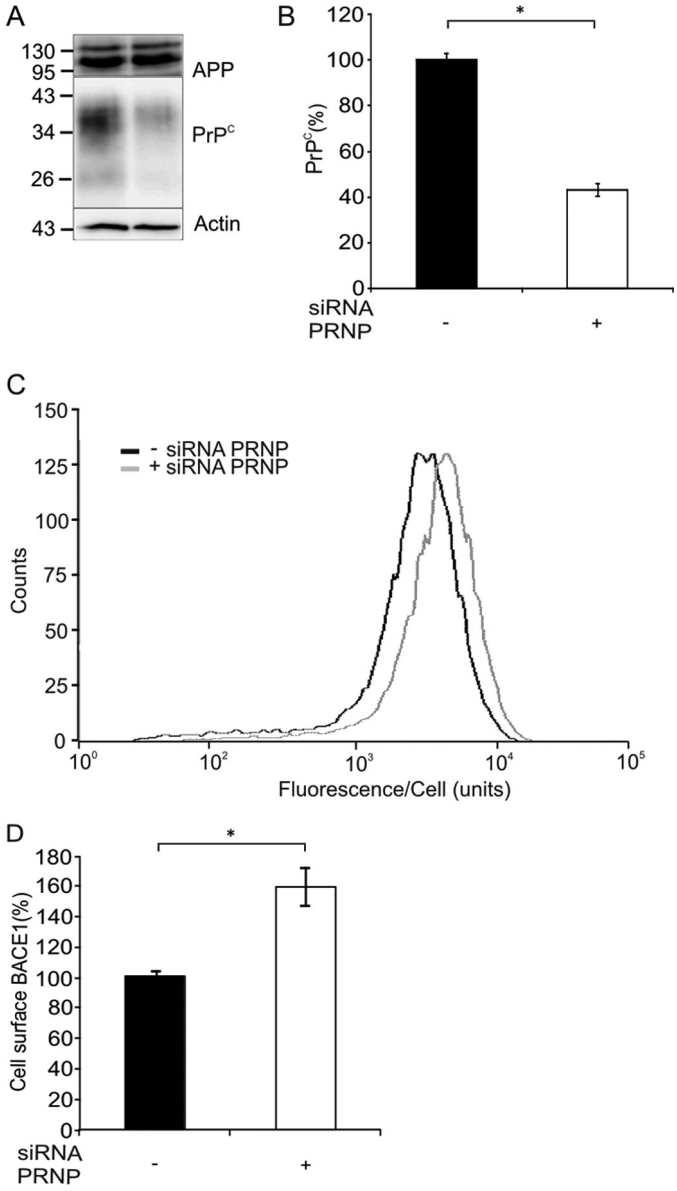


FIGURE 4. **siRNA knockdown of endogenous PrP$^C$ increases cell surface localization of BACE1.** *A*, siRNA knockdown of endogenous PrP$^C$ in HEK293 cells. Lysates were subjected to SDS-PAGE and immunoblotting to detect endogenous APP, PrP$^C$, and actin. *B*, endogenous BACE1 cell surface fluorescence in the presence and after knockdown of endogenous PrP$^C$ as determined by FACS analysis. *C*, quantitation from FACS analysis of BACE1 surface fluorescence following siRNA knockdown of PrP$^C$ ($n = 9$). *, $p < 0.05$; *error bars*, ±S.E.

but did not alter the amount of BACE1 colocalized with the ER marker calreticulin (Fig. 3, *G* and *H*). Together, these results indicate that the interaction of PrP$^C$ with the prodomain of BACE1 slows its trafficking following its exit from the ER, increasing its localization in the TGN and thereby reducing the amount at the cell surface and in endosomes.

To confirm that the above results were not caused by forced interactions due to overexpression of the proteins, we used FACS analysis to determine the surface level of endogenous BACE1 in HEK293 cells following siRNA knockdown of endogenous PrP$^C$ (Fig. 4*A*). Knockdown of endogenous PrP$^C$ (Fig. 4*B*) resulted in a 151% increase in the amount of endogenous BACE1 at the cell surface (Fig. 4, *C* and *D*). Together with the coimmunoprecipitation experiments of endogenous proteins in brain (Fig. 1*A*), these results indicate that the interaction between BACE1 and PrP$^C$ is of physiological relevance and has a physiological effect.

*Deletion of PrP$^C$ Does Not Affect APP Processing or Aβ Deposition in Mouse Model*—We extended our analysis of PrP$^C$ function in AD by examining the effect of PrP$^C$ deletion on Aβ production and deposition in a transgenic mouse model expressing human APP. PrP$^C$-null 129/Ola mice (22) were crossed with mice expressing human APP with APP$_{Swe,Ind}$ (25). Immunoblot analysis confirmed the lack of PrP$^C$ in the APP$_{Swe,Ind}$/PrP$^{-/-}$ mice (Fig. 5, *A* and *B*); however, PrP$^C$ deletion had no effect on the level of sAPPβ$_{Swe}$ (Fig. 5, *A* and *B*). Histopathological analysis indicated that there was no apparent difference in thioflavin S fluorescence (Fig. 5*C*) or in total Aβ plaque load (Fig. 5*D*) in the hippocampus between the APP$_{Swe,Ind}$/PrP$^{-/-}$ mice and the APP$_{Swe,Ind}$/PrP$^{+/+}$ mice. As oligomeric forms of Aβ more closely correlate with cognitive dysfunction than Aβ plaque load (31), we investigated whether depletion of PrP$^C$ affected the level of prefibrillar Aβ oligomers using the A11 antibody (32) and fibrillar Aβ oligomers using the OC antibody (33). However, no apparent differences in the level of prefibrillar Aβ oligomers detected with the A11 antibody (Fig. 5*E*) or in fibrillar Aβ oligomers detected with the OC antibody (Fig. 5*F*) were observed between the APP$_{Swe,Ind}$/PrP$^{-/-}$ and the APP$_{Swe,Ind}$/PrP$^{+/+}$ mice. Further analysis revealed that there was no difference in the amount of soluble (SDS-extracted) Aβ(1–40) and Aβ(1–42) (Fig. 5*G*) in the APP$_{Swe,Ind}$/PrP$^{-/-}$ mice compared with the APP$_{Swe,Ind}$/PrP$^{+/+}$ mice at either 20 or 40 weeks of age. There were small but significant increases in the amount of insoluble (formic acid-extracted) Aβ(1–40) at 40 weeks (Fig. 5*H*) and in the amount of insoluble Aβ(1–42) at both 20 and 40 weeks (Fig. 5*H*) in the APP$_{Swe,Ind}$/PrP$^{-/-}$ mice compared with the APP$_{Swe,Ind}$/PrP$^{+/+}$ mice. Furthermore, deletion of PrP$^C$ had no apparent effect on the synaptic immunoreactivity of synaptophysin or drebrin or on microglial or astrocyte activation in the hippocampus (supplemental Fig. S1, A–D). In addition, immunoblot analysis revealed that there was no significant difference in the levels of the synaptic proteins synaptophysin, PSD95, and drebrin in the APP$_{Swe,Ind}$/PrP$^{-/-}$ mice compared with the APP$_{Swe,Ind}$/PrP$^{+/+}$ mice (supplemental Fig. S1, E and F). Also, there was no difference in the level of the γ-secretase complex components presenilin-1 and nicastrin in the APP$_{Swe,Ind}$/PrP$^{-/-}$ mice compared with the APP$_{Swe,Ind}$/PrP$^{+/+}$ mice (supplemental Fig. S1, E and F). Finally, we investigated whether the lack of effect of PrP$^C$ depletion on Aβ deposition was due to an increase in Aβ degradation by examining the levels of the Aβ-degrading enzymes neprilysin and insulin-degrading enzyme. However, no significant difference in the levels of these two enzymes was observed between the APP$_{Swe,Ind}$/PrP$^{-/-}$ and the APP$_{Swe,Ind}$/PrP$^{+/+}$ mice (supplemental Fig. S1, E and F), indicating that the lack of effect of PrP$^C$ deletion on Aβ deposition was unlikely due to an increase in Aβ degradation. Taken together, these extensive biochemical and histopathological analyses indicate that deletion of PrP$^C$ does not modulate the deposition of Aβ in this APP$_{Swe,Ind}$ transgenic mouse model.

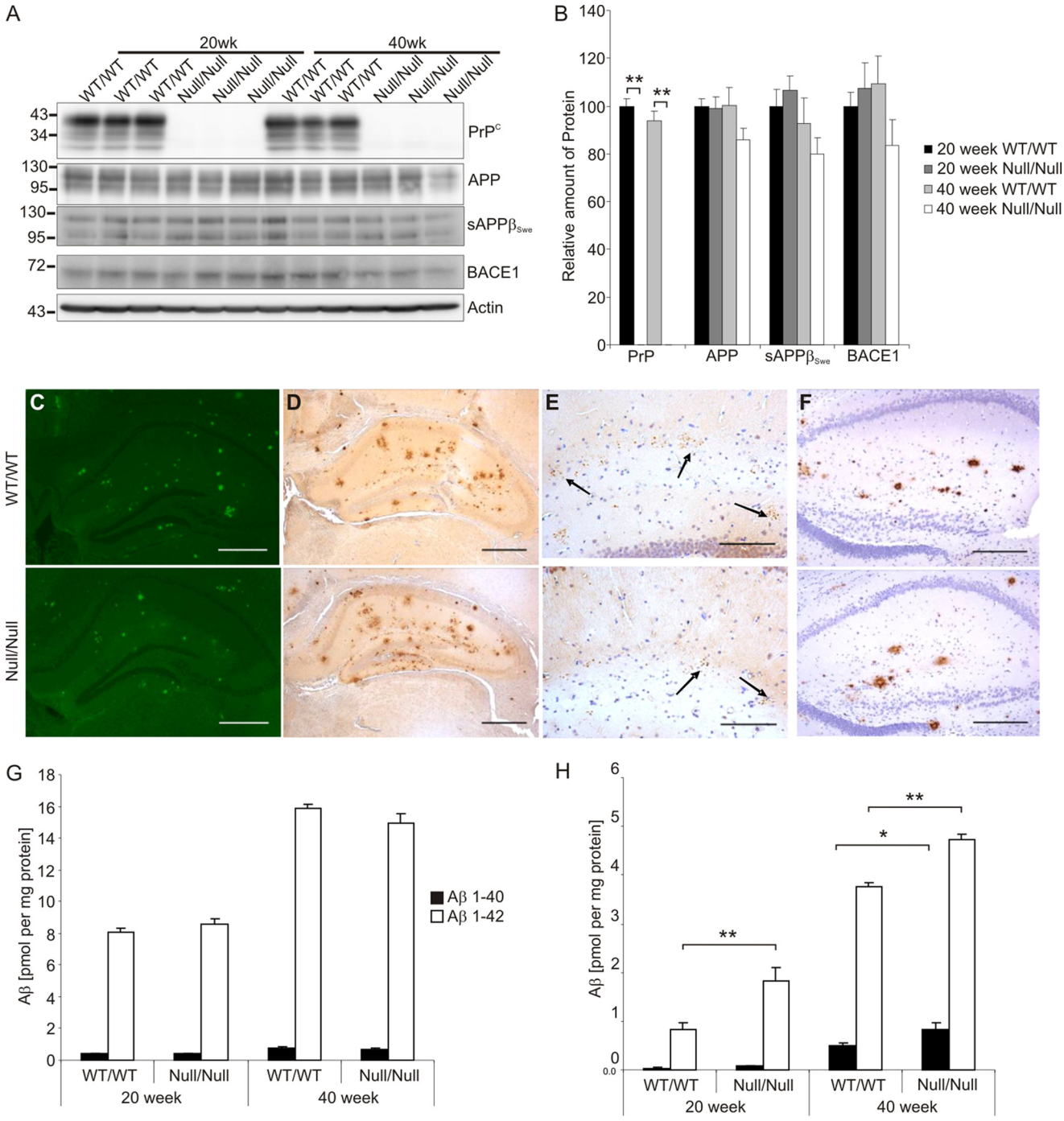


FIGURE 5. **PrP$^C$ deletion does not affect APP processing or Aβ deposition in transgenic mouse model.** Brain hemispheres from 20- and 40-week APP$_{Swe,Ind}$/PrP$^{+/+}$ (*WT/WT*) and APP$_{Swe,Ind}$/PrP$^{-/-}$ (*Null/Null*) mice were homogenized using a two-step protocol, and the SDS-soluble fraction was subjected to SDS-PAGE and immunoblotting. *A*, representative blots of PrP$^C$, APP, sAPPβ$_{Swe}$, and BACE1 with actin as a loading control. *B*, relative amounts of protein determined by densitometric analysis ($n = 6$). *C–F*, histological analysis of the cerebrum of APP$_{Swe,Ind}$/PrP$^{+/+}$ (*WT/WT*) and APP$_{Swe,Ind}$/PrP$^{-/-}$ (*Null/Null*) mice showing Aβ amyloid deposits. *C*, thioflavin S fluorescent aggregates. *D*, Aβ-immunoreactive aggregates detected with antibody 4G8. *E*, Aβ oligomeric deposits (*arrows*) detected with antibody A11. *F*, Aβ oligomeric deposits detected with antibody OC. *Scale bars*, 400 μm in *C* and *D*, 100 μm in *E*, and 200 μm in *F*. Soluble (SDS-extracted) Aβ(1–40) and Aβ(1–42) (*G*) and insoluble (formic acid-extracted) Aβ(1–40) and Aβ(1–42) (*H*) detected by ELISA ($n = 7–9$) are shown. *, $p < 0.05$; **, $p < 0.005$; *error bars*, ±S.E.

*PrP$^C$ Differentially Affects Metabolism of APP$_{WT}$ and APP$_{Swe}$*—Our previous observations showed that PrP$^C$ inhibited the activity of BACE1 toward human APP$_{WT}$ in cellular models and toward murine APP$_{WT}$ in PrP-null mice (10). To reconcile these observations with the lack of effect of deletion of PrP$^C$ on Aβ production and deposition in the APP$_{Swe,Ind}$ transgenic mice, we considered whether this was due to the Swedish double point mutation K670N/M671L N-terminal to the BACE1 cleavage site. To investigate this, the effect of PrP$^C$ on Aβ production was examined in HEK293 cells stably expressing either APP$_{WT}$ (Fig. 6*A*) or APP$_{Swe}$ (Fig. 6*B*). PrP$^C$ dramatically reduced the secretion of Aβ(1–40) and Aβ(1–42) from the

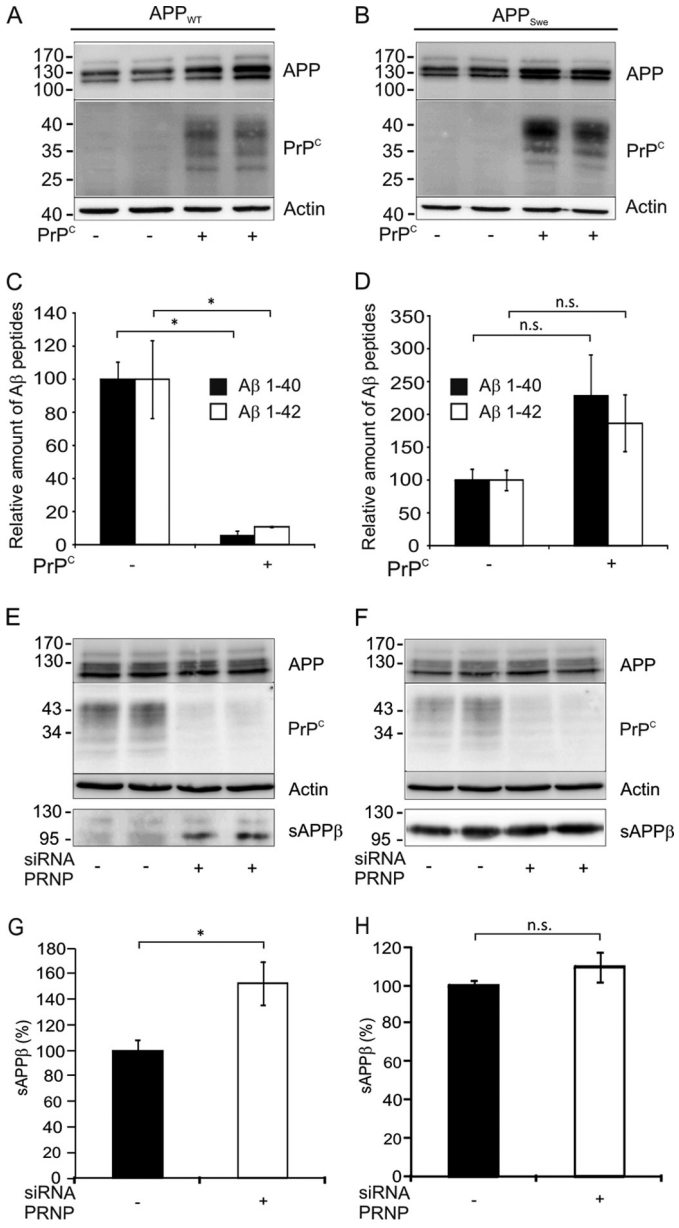


FIGURE 6. **PrP$^C$ does not inhibit production of Aβ from cells expressing APP$_{Swe}$.** Lysates from HEK293 cells expressing either APP$_{WT}$ (*A*) or APP$_{Swe}$ (*B*) in the presence or absence or PrP$^C$ were subjected to SDS-PAGE and immunoblotting to detect PrP$^C$, APP, and actin. Medium from HEK293 cells expressing either APP$_{WT}$ ($n = 3$) (*C*) or APP$_{Swe}$ ($n = 6$) (*D*) in the presence or absence or PrP$^C$ was subjected to ELISA to detect Aβ(1–40) and Aβ(1–42). Lysates from HEK293 cells expressing either APP$_{WT}$ (*E*) or APP$_{Swe}$ (*F*) in which endogenous PrP$^C$ had been knocked down by siRNA were subjected to SDS-PAGE and immunoblotting to detect APP, endogenous PrP$^C$, and actin. Medium samples were blotted for sAPPβ. Quantification by densitometric analysis of multiple immunoblots of sAPPβ from APP$_{WT}$ (*G*) or APP$_{Swe}$ (*H*) in the presence or absence of *PRNP* siRNA ($n = 4$) is shown. *, $p < 0.05$; *n.s.*, not significant; *error bars*, ±S.E.

cells expressing APP$_{WT}$ (Fig. 6*C*), consistent with our previous data in other cell lines (10). However, there was no inhibitory effect of PrP$^C$ on the secretion of the Aβ peptides from the cells expressing APP$_{Swe}$ (Fig. 6*D*). To confirm this result, we performed the converse experiment using siRNA to knock down the endogenous PrP$^C$ in the HEK293 cells expressing either APP$_{WT}$ (Fig. 6*E*) or APP$_{Swe}$ (Fig. 6*F*). Knockdown of PrP$^C$ resulted in an increase in sAPPβ in the cells expressing APP$_{WT}$ (Fig. 6*G*) but had no effect in the cells expressing APP$_{Swe}$ (Fig. 6*H*). These data clearly show that PrP$^C$ differentially affects the activity of BACE1 toward APP$_{WT}$ and APP$_{Swe}$.

## DISCUSSION

We have reported previously that PrP$^C$ inhibits the BACE1 cleavage of APP$_{WT}$ and that deletion of PrP$^C$ in both cell and animal model systems resulted in an increase in endogenous Aβ levels (10). From this, we proposed that a normal function of PrP$^C$ may be to regulate the production of the neurotoxic Aβ and therefore to protect against AD (11). In the present study, we have extended these observations by determining the molecular and cellular mechanisms involved in the regulation of BACE1 by PrP$^C$. Here, we show that PrP$^C$ interacts directly with the prodomain of the immature, Golgi-localized form of BACE1 and that Pro$^{29}$ in the prodomain is critical for this interaction.

Prodomain cleavage, which occurs in the TGN by furin-like convertases, is required for the generation of mature BACE1 (13–16). The mature BACE1 is present at the cell surface from where it is internalized into endosomes where it preferentially cleaves APP$_{WT}$ (6). Our data show that PrP$^C$ interacts with the prodomain of BACE1 and that Pro$^{29}$ in the prodomain appears to be critical for this protein-protein interaction. This interaction of PrP$^C$ with the immature prodomain-containing form of BACE1 results in an increased proportion of the secretase in the TGN with a subsequent reduction in the amount at the cell surface and in endosomes. We propose that this retention of BACE1 in the secretory pathway provides a mechanism to explain the inhibitory effect of PrP$^C$ on the amyloidogenic processing of APP$_{WT}$, which is cleaved by BACE1 in endosomes (14, 17–19). Although there is only an approximately 30% reduction in BACE1 localization to the endosomes, this is enough to nearly abolish the generation of Aβ. It is unlikely that the total cellular pool of BACE1 is intended for localization to the appropriate subcellular compartments for processing of APP$_{WT}$ as BACE1 is required for the processing of several other substrates (34).

The mechanism of action of PrP$^C$ on BACE1 processing of APP is reminiscent of that of the sorting protein-related receptor, which also inhibits the proteolytic processing of APP and production of Aβ (35). Like PrP$^C$, sorting protein-related receptor coimmunoprecipitated only with the smaller prodomain-containing immature form of BACE1, suggesting an interaction in the Golgi (36). However, unlike sorting protein-related receptor, which also interacts with APP, impairing its transport through the Golgi and blocking access of APP to BACE1 (35, 36), PrP$^C$ does not interact with APP (10).

We also sought to confirm a role for PrP$^C$ upstream of Aβ production by examining the effect of deletion of PrP$^C$ in a transgenic mouse model expressing mutant human APP. For this purpose, we chose the widely used J20 transgenic mouse model, which expresses human APP with the Swedish and Indiana mutations under the control of the platelet-derived growth factor (PDGF) promoter (25). Surprisingly, despite extensive biochemical and histopathological analysis, we could find no evidence for an affect of PrP$^C$ deletion on APP proteolytic processing, Aβ plaque deposition, or levels of soluble Aβ or Aβ

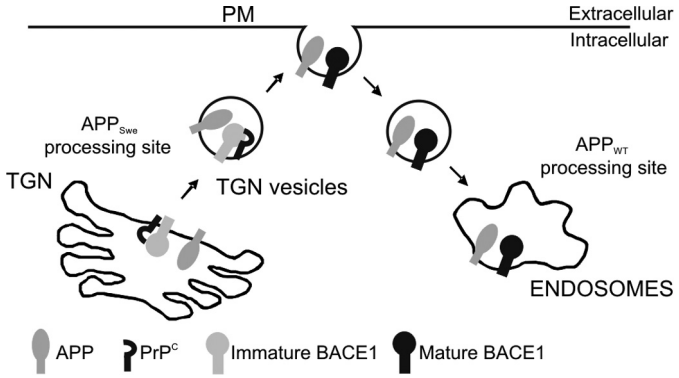


FIGURE 7. **Schematic diagram showing differential effect of PrP$^C$ on cleavage of APP$_{WT}$ and APP$_{Swe}$ by BACE1.** PrP$^C$ interacts with the prodomain of BACE1 in its immature form in the TGN, slowing its maturation and trafficking to the cell surface and subsequent internalization into endosomes. In the TGN, BACE1 preferentially cleaves APP$_{Swe}$; in the endosomes, it preferentially cleaves APP$_{WT}$. *PM*, plasma membrane.

oligomers. Consistent with our observations in the APP$_{Swe,Ind}$ (J20) transgenic mice, it has also been reported recently that deletion of PrP$^C$ failed to alter BACE1 processing of APP, A$\beta$ levels, and A$\beta$ deposition in the APP$_{Swe}$/PS1$_{\Delta E9}$ (37) and the APP$_{Swe}$PS1$_{L166P}$ (38) transgenic models and previously that overexpression of PrP$^C$ in APP$_{Swe,Ind}$ transgenic mice resulted in only a minor increase in A$\beta$ plaque formation but no significant change in A$\beta$(1–40) or A$\beta$(1–42) (39). However, considering that APP$_{WT}$ is primarily cleaved by BACE1 in endosomes (17–19), whereas the cleavage of APP$_{Swe}$ occurs primarily within the TGN (20, 21), our current data indicating that PrP$^C$ interacts directly with the prodomain of BACE1, retaining BACE1 in the TGN and decreasing its amount in endosomes, provide a cellular mechanism to explain the differential effect of PrP$^C$ on APP$_{WT}$ and APP$_{Swe}$ metabolism (Fig. 7). Thus, the differential subcellular sites of action of BACE1 on APP$_{WT}$ (in endosomes) compared with APP$_{Swe}$ (in the TGN) can explain the lack of effect of PrP$^C$ deletion on APP processing and A$\beta$ deposition in the APP$_{Swe,Ind}$/PrP$^{-/-}$ mice. The dramatically different effect of PrP$^C$ on the BACE1 cleavage of APP$_{WT}$ and APP$_{Swe}$ in HEK cells confirms this.

Clearly, animal models based on the rare familial AD mutations in APP have played a major role in defining disease-related mechanisms and in evaluating novel therapeutic approaches (1). However, a recent report highlighted the potential limitation of such models when the decreased potency of BACE1 inhibitors in cells and mice expressing APP$_{Swe}$ was shown to be due to the different subcellular location of APP$_{Swe}$ processing by BACE1 (40), similar to our observations here on the differential effect of PrP$^C$ on the metabolism of APP$_{WT}$ and APP$_{Swe}$ by BACE1. Consistent with our hypothesis that PrP$^C$ regulates the metabolism of APP$_{WT}$ is the finding that PrP$^C$ is decreased in the hippocampus and temporal cortex in sporadic AD but not in familial AD, indicating that the reduction in PrP$^C$ would appear to reflect a primary mechanism of disease and is not merely a secondary consequence of other AD-associated changes (12). Although PrP$^C$ exerts no control on cleavage of APP$_{Swe}$ that is associated with familial AD, it has a profound influence on the cleavage of APP$_{WT}$, and together with other data (12), this suggests that PrP$^C$ may be a key protective player against sporadic AD.

*Acknowledgments—We thank C. Troakes, S. Al-Sarraj, and M. Rossor of the Medical Research Council London Neurodegenerative Diseases Brain Bank for provision of samples. We thank Sian Hilton for assistance in making the BACE1 mutants, Dr. Gareth Howell for assistance with the FACS analysis, Mary Brady for animal care, Sandra Mack and Gillian McGregor for cutting the histology sections, Dr. Liz Eckman, and Dr. Pritam Das for provision of the A$\beta$ ELISA antibodies.*

## REFERENCES

1. Morrissette, D. A., Parachikova, A., Green, K. N., and LaFerla, F. M. (2009) *J. Biol. Chem.* **284,** 6033–6037
2. Mullan, M., Crawford, F., Axelman, K., Houlden, H., Lilius, L., Winblad, B., and Lannfelt, L. (1992) *Nat. Genet.* **1,** 345–347
3. Murrell, J., Farlow, M., Ghetti, B., and Benson, M. D. (1991) *Science* **254,** 97–99
4. Selkoe, D. J. (2001) *Physiol. Rev.* **81,** 741–766
5. Vardy, E. R., Catto, A. J., and Hooper, N. M. (2005) *Trends Mol. Med.* **11,** 464–472
6. Cole, S. L., and Vassar, R. (2008) *J. Biol. Chem.* **283,** 29621–29625
7. Fukumoto, H., Cheung, B. S., Hyman, B. T., and Irizarry, M. C. (2002) *Arch. Neurol.* **59,** 1381–1389
8. Li, R., Lindholm, K., Yang, L. B., Yue, X., Citron, M., Yan, R., Beach, T., Sue, L., Sabbagh, M., Cai, H., Wong, P., Price, D., and Shen, Y. (2004) *Proc. Natl. Acad. Sci. U.S.A.* **101,** 3632–3637
9. Vassar, R., Kovacs, D. M., Yan, R., and Wong, P. C. (2009) *J. Neurosci.* **29,** 12787–12794
10. Parkin, E. T., Watt, N. T., Hussain, I., Eckman, E. A., Eckman, C. B., Manson, J. C., Baybutt, H. N., Turner, A. J., and Hooper, N. M. (2007) *Proc. Natl. Acad. Sci. U.S.A.* **104,** 11062–11067
11. Hooper, N. M., and Turner, A. J. (2008) *Trends Biochem. Sci.* **33,** 151–155
12. Whitehouse, I. J., Jackson, C., Turner, A. J., and Hooper, N. M. (2010) *J. Alzheimers Dis.* **22,** 1023–1031
13. Bennett, B. D., Denis, P., Haniu, M., Teplow, D. B., Kahn, S., Louis, J. C., Citron, M., and Vassar, R. (2000) *J. Biol. Chem.* **275,** 37712–37717
14. Capell, A., Steiner, H., Willem, M., Kaiser, H., Meyer, C., Walter, J., Lammich, S., Multhaup, G., and Haass, C. (2000) *J. Biol. Chem.* **275,** 30849–30854
15. Benjannet, S., Elagoz, A., Wickham, L., Mamarbachi, M., Munzer, J. S., Basak, A., Lazure, C., Cromlish, J. A., Sisodia, S., Checler, F., Chrétien, M., and Seidah, N. G. (2001) *J. Biol. Chem.* **276,** 10879–10887
16. Creemers, J. W., Ines Dominguez, D., Plets, E., Serneels, L., Taylor, N. A., Multhaup, G., Craessaerts, K., Annaert, W., and De Strooper, B. (2001) *J. Biol. Chem.* **276,** 4211–4217
17. Vassar, R., Bennett, B. D., Babu-Khan, S., Kahn, S., Mendiaz, E. A., Denis, P., Teplow, D. B., Ross, S., Amarante, P., Loeloff, R., Luo, Y., Fisher, S., Fuller, J., Edenson, S., Lile, J., Jarosinski, M. A., Biere, A. L., Curran, E., Burgess, T., Louis, J. C., Collins, F., Treanor, J., Rogers, G., and Citron, M. (1999) *Science* **286,** 735–741
18. Huse, J. T., Pijak, D. S., Leslie, G. J., Lee, V. M., and Doms, R. W. (2000) *J. Biol. Chem.* **275,** 33729–33737
19. Yan, R., Han, P., Miao, H., Greengard, P., and Xu, H. (2001) *J. Biol. Chem.* **276,** 36788–36796
20. Haass, C., Lemere, C. A., Capell, A., Citron, M., Seubert, P., Schenk, D., Lannfelt, L., and Selkoe, D. J. (1995) *Nat. Med.* **1,** 1291–1296
21. Thinakaran, G., Teplow, D. B., Siman, R., Greenberg, B., and Sisodia, S. S. (1996) *J. Biol. Chem.* **271,** 9390–9397
22. Manson, J. C., Clarke, A. R., Hooper, M. L., Aitchison, L., McConnell, I., and Hope, J. (1994) *Mol. Neurobiol.* **8,** 121–127
23. Zhao, J., Fu, Y., Yasvoina, M., Shao, P., Hitt, B., O'Connor, T., Logan, S., Maus, E., Citron, M., Berry, R., Binder, L., and Vassar, R. (2007) *J. Neurosci.*

**27,** 3639–3649
24. Walmsley, A. R., Zeng, F., and Hooper, N. M. (2001) *EMBO J.* **20,** 703–712
25. Mucke, L., Masliah, E., Yu, G. Q., Mallory, M., Rockenstein, E. M., Tatsuno, G., Hu, K., Kholodenko, D., Johnson-Wood, K., and McConlogue, L. (2000) *J. Neurosci.* **20,** 4050–4058
26. Piccardo, P., Manson, J. C., King, D., Ghetti, B., and Barron, R. M. (2007) *Proc. Natl. Acad. Sci. U.S.A.* **104,** 4712–4717
27. Kawarabayashi, T., Younkin, L. H., Saido, T. C., Shoji, M., Ashe, K. H., and Younkin, S. G. (2001) *J. Neurosci.* **21,** 372–381
28. Haugabook, S. J., Yager, D. M., Eckman, E. A., Golde, T. E., Younkin, S. G., and Eckman, C. B. (2001) *J. Neurosci. Methods* **108,** 171–179
29. Bennett, B. D., Babu-Khan, S., Loeloff, R., Louis, J. C., Curran, E., Citron, M., and Vassar, R. (2000) *J. Biol. Chem.* **275,** 20647–20651
30. Sun, X., He, G., and Song, W. (2006) *FASEB J.* **20,** 1369–1376
31. Walsh, D. M., and Selkoe, D. J. (2007) *J. Neurochem.* **101,** 1172–1184
32. Kayed, R., Head, E., Thompson, J. L., McIntire, T. M., Milton, S. C., Cotman, C. W., and Glabe, C. G. (2003) *Science* **300,** 486–489
33. Kayed, R., Head, E., Sarsoza, F., Saing, T., Cotman, C. W., Necula, M., Margol, L., Wu, J., Breydo, L., Thompson, J. L., Rasool, S., Gurlo, T., Butler, P., and Glabe, C. G. (2007) *Mol. Neurodegener.* **2,** 18
34. Cole, S. L., and Vassar, R. (2007) *Mol. Neurodegener.* **2,** 22
35. Andersen, O. M., Reiche, J., Schmidt, V., Gotthardt, M., Spoelgen, R., Behlke, J., von Arnim, C. A., Breiderhoff, T., Jansen, P., Wu, X., Bales, K. R., Cappai, R., Masters, C. L., Gliemann, J., Mufson, E. J., Hyman, B. T., Paul, S. M., Nykjaer, A., and Willnow, T. E. (2005) *Proc. Natl. Acad. Sci. U.S.A.* **102,** 13461–13466
36. Spoelgen, R., von Arnim, C. A., Thomas, A. V., Peltan, I. D., Koker, M., Deng, A., Irizarry, M. C., Andersen, O. M., Willnow, T. E., and Hyman, B. T. (2006) *J. Neurosci.* **26,** 418–428
37. Gimbel, D. A., Nygaard, H. B., Coffey, E. E., Gunther, E. C., Laurén, J., Gimbel, Z. A., and Strittmatter, S. M. (2010) *J. Neurosci.* **30,** 6367-6374
38. Calella, A. M., Farinelli, M., Nuvolone, M., Mirante, O., Moos, R., Falsig, J., Mansuy, I. M., and Aguzzi, A. (2010) *EMBO Mol. Med.* **2,** 306–314
39. Schwarze-Eicker, K., Keyvani, K., Görtz, N., Westaway, D., Sachser, N., and Paulus, W. (2005) *Neurobiol. Aging* **26,** 1177–1182
40. Yamakawa, H., Yagishita, S., Futai, E., and Ishiura, S. (2010) *J. Biol. Chem.* **285,** 1634–1642